Actively lubricated hybrid journal bearings based on magnetic fluids for high-precision spindles of machine tools

Luis Norberto Lopez de Lacalle, Harkaitz Urreta, Gorka Aguirre, Pavel Kuzhir, Luis Norberto López de Lacalle

Actively lubricated hybrid journal bearings based on magnetic fluids for high precision spindles of machine tools

Harkaitz Urreta[1]*, Gorka Aguirre[1], Pavel Kuzhir[2], Luis Norberto Lopez de Lacalle[3]

1 IK4-IDEKO, Arriaga 2, E-20870 Elgoibar, Spain

2 University Côte d'Azur, CNRS UMR 7010 Inst. of Physics of Nice, Parc Valrose 06100 Nice, France

3 EHU-UPV Dept. Mechanical Engineering, Alameda Urquijo S/N, E-48013 Bilbao, Spain

* Corresponding author hurreta@ideko.es; Tel: +34943748000 ; Fax: +34943743804

Abstract

The research work reported in this paper is focused on the use of magnetic fluids as active lubricant for improving the performance of hybrid journal bearings, with application to high precision machine tools. Prototype design was optimized following numerical computation of Reynolds equation and computational fluid dynamics (CFD) calculations, in both cases with Herschel-Buckley model for the magnetorheological fluid. This fluid (LORD Corp. MRF 122-2ED) was experimentally characterized in detail. The improvement of the hydrodynamic effect in journal bearings was demonstrated with 50% higher load capacity and stiffness, mainly at half of shaft eccentricity $0.4<\varepsilon<0.7$. Active hydrostatic lubrication achieved quasi-infinite stiffness within working limits (load and speed), at low frequencies. For high dynamic response the active lubrication based on magnetorheological valves did not show good response. The feasibility of using magnetic fluids for developing high performance machine tool spindles and the validity of the simulation models was demonstrated experimentally.

Keywords

Magnetorheological fluid, MR valves, active bearing, CFD, machine tool, spindle.

Nomenclature and main variables

b	Recess width	[m]	S	Stiffness	[N/m]
B	Magnetic flux density	[T]	t	Time	[s]
C	Radial clearance	[m]	T	Temperature	[ºC]
F	Force	[N]	W	Load capacity	[N]
F_f	Friction force	[N]	x,y,z	Linear coordinates	[-]
h	Film thickness	[m]	r,θ,z	Cylind. coordinates	[-]
H	Magnetic field strength	[A/m]	u,v,w	Fluid velocity	[m/s]
l	Recess length	[m]	$\dot{\gamma}$	Shear rate	[1/s]
L	Bearing length	[m]	θ	Angular coordinate	[º]
n	Number of pockets	[-]	ρ	Density	[kg/m^3]
p	Pressure distribution	[Pa]	σ	Stress	[Pa]
P_r	Recess pressure	[Pa]	τ	Shear stress	[Pa]
P_p	Pumping pressure	[Pa]	μ	Dynamic viscosity	[Pa·s]
Q	Flowrate	[m^3/s]	ν	Kinematic viscosity	[m^2/s]
R	Radius	[m]	ϕ	Attitude angle	[º]
R_a	Shaft radius	[m]	ψ	Angular abscissa	[º]
R_c	Bearing raius	[m]	Ω	Angular speed	[1/s]
R_h	Hydraulic resistance	[$Pa\cdot s/m^3$]			
R_o	Hydraulic resist. bearing	[$Pa\cdot s/m^3$]			
R_i	Hydraulic resist. restrictor	[$Pa\cdot s/m^3$]			

$\beta = \frac{1}{1+R_i/R_o}$	Hydraulic resistance ratio	$\lambda = \frac{L}{2R}$	Length to diameter ratio
$\varepsilon = \frac{e}{R}$	Relative eccentricity	$\tau_0^* = \frac{\tau_0 C}{\mu_0 R\omega}$	Dimensionless yield stress
$\Delta X = \frac{\Delta x}{R}$	Dimensionless element size in tangential direction	$H = \frac{h}{C}$	Dimensionless gap size
$\Delta Y = \frac{\Delta h}{h}$	Dimensionless element size in radial direction	$P = \frac{p(C/R)^2}{\mu\omega}$	Dimensionless pressure
$\Delta Z = \frac{\Delta z}{L}$	Dimensionless element size in axial direction	$\frac{dP}{dX} = \frac{dp}{dx}\frac{(C/R)^2}{\mu\omega}$	Dimensionless pressure gradient tangential
$u = \frac{v_x}{\omega R}$	Dimensionless velocity in tangential direction	$\frac{dP}{dZ} = \frac{dp}{dz}\frac{(C/R)^2}{\mu\omega}$	Dimensionless pressure gradient axial
$w = \frac{v_z}{\omega R}$	Dimensionless velocity in axial direction		

INTRODUCTION

The introduction to this research work has three sections, 1) a brief introduction to classic lubricated bearings with hydrostatic and hydrodynamic lubrication, 2) active bearings and 3) active hybrid journal bearings with magnetic fluid.

Hydrostatic and hydrodynamic lubrication bearings

Pressurized lubricated bearings, commonly known as hydrostatic or hydrodynamic bearings, are quite widely used and known by manufacturers of high-precision machine tools. Most influencing authors in the machine tool building field, for instance M. Weck (Weck, 1984), agree that between the available technologies for guiding systems, namely sliding, rolling and pressurized lubricant technologies, the latter offers better properties, considering resolution, damping and smoothness in the movement. Lubricated bearings can work in either hydrostatic or hydrodynamic regime, in function of the boundary conditions, i.e.: external oil pressurization, geometry of the bearing, fluid viscosity and applied load.

Hydrodynamic bearings, where pressure is generated by relative motion between the bearing surfaces (Frêne et al., 1997), are suitable for applications where working conditions are quite stationary. Thus, with a proper design of the bearing, a stable and safe pressurized oil thin film can be achieved between the moving parts, the shaft and the bearing, avoiding any contact, friction and therefore wear. The pressure in the bearing follows the classic equation in thin fluid films proposed by Osborne Reynolds (Reynolds, 1886). The main hydrodynamic bearing drawback are the starting and deceleration stages, where fluid velocity is so low that lubricant film cannot support the load, leading to contact, friction and wear of surfaces.

To avoid contact and wear whatever is relative movement speed, hydrostatic lubrication (Bassani and Piccigallo, 1992) is the proper solution. In this case, lubricant fluid pressure is provided by an external hydraulic pump, which ensures a fully developed thin lubricant film between bearing and shaft. The bearing behaviour is strongly dependent on the selection of compensation valves, commonly known as *restrictors*. Restrictors determine fundamental mechanical properties of the bearing, like stiffness and force. With increasing shaft speed, hydrodynamic pressure appears in the hydrostatic bearings, as described by Reynolds equation. Hydrostatic bearings can thus, in function of the geometry, oil viscosity and operational conditions, become in a "hybrid bearing" with mixed hydrodynamic and hydrostatic lubrication regime. Figure 1 scheme shows the bearing hydrodynamic pressure governed by Reynolds equation (1).

[insert figure 1]

Figure 1 Hydrodynamic pressure in journal bearings.

$$\frac{\partial}{\partial x}\left(\frac{\rho h^3}{\mu}\frac{\partial p}{\partial x}\right)+\frac{\partial}{\partial z}\left(\frac{\rho h^3}{\mu}\frac{\partial p}{\partial z}\right)=6\rho\left(U_1+U_2\right)\frac{\partial h}{\partial x}+6\rho h\frac{\partial}{\partial x}\left(U_1-U_2\right)+12\rho V+12\dot{\rho}h \qquad (1)$$

Figure 2 shows the implementation of hydrostatic lubrication ruled by the basic equations (2).

[insert figure 2]

Figure 2 Hybrid journal bearing and hydraulic circuit

$$P_r=\beta\cdot P_p=\frac{1}{1+{}^{R_i}/_{R_o}}\cdot P_p \qquad W=\int_{-L}^{+L}\int_{-\pi}^{+\pi}p\cdot dA \qquad S=\frac{dW}{d\varepsilon} \qquad (2)$$

The improvement of the performance of journal bearing with hybrid lubrication by means of active magnetic fluids will be discussed in this paper.

Active bearings for smart systems

Following Reynolds and hydrostatic lubrication basic equations, see Eqs. (1) and (2), an active lubricated bearing can be achieved by the modification of bearing geometry, fluid viscosity and/or restrictor hydraulic resistance, the latter in the case of hydrostatic bearings.

Geometry change is a very complex option due the requirement of a mechanism to produce micrometric deformation with as large as possible stiffness. This solution has been explored with active air bearings by including flexible structures driven by piezo actuators (Aguirre et al., 2010; Morosi and Santos, 2011; Shamoto et al., 2006), but they are not transposable to high pressure hybrid journal bearings. Working with oil lubricated bearings, different approaches can be found in bibliography for pure hydrodynamic cases, e.g. closed loop control in oil feeding (Albers et al., 2011) to improve the energy efficiency of guiding, and in the particular case of tilting pads hydrodynamic bearings (Deckler, 2004; Nicoletti and Santos, 2003; Sun and Krodkiewski, 1999), the lubrication conditions and tilting angle of pads were modified by hydraulic or electromechanical actuators.

Regarding active bearings with hydrostatic lubrication, therefore with active restrictors (Jordan, 2000), some other research works aimed at a) the improvement of hybrid bearings with servo-valves (Santos and Watanabe, 2006), b) the study of active lubrication in complex multibody simulation (Estupiñan and Santos, 2009), and c) special considerations required for flexible rotors typical of energy generation machinery (Nicoletti and Santos, 2008). But a common characteristic in all those works was either the use of complex mechanisms for the bearing, or precise servo-valves for lubricant feeding.

Active hybrid lubricated bearings with magnetic fluids

A second research strand about actively lubricated bearings was focused on the use of fluids with rheological response under external exciting fields: electro-rheological fluids and magnetic fluids.

Electrorheological fluids change their rheology under electric field, increasing the shear stress proportionally to the field. Some research works developed active bearings (hydrodynamic and hydrostatic) using this kind of fluid as lubricant, e.g. in high-speed journal bearings to control stiffness and stability (G. Nikolakopoulos and Papadopoulos, 1998), describing the theoretical behaviour of journal bearings lubricated with active fluids (Peng and Zhu, 2005), and studying the use of electrorheological fluids for active hydrostatic bearings (Bouzidane et al., 2008). In all those cases the high voltage (in the range of 1-10kV) electric field required achieve a high enough electrorheological effect was reported as a serious drawback for industrial implementation.

Regarding magnetic fluids, two main groups can be noted: ferrofluids and magnetorheological fluids, hereinafter MRF. All magnetic fluids are composed by a carrier fluid (lubricant oil in this case), additives to improve tribology and fluid stability, and magnetic particles, which in function of their size (nanometric or micrometric) define their behaviour. Ferrofluids contain stabilized nanometric particles (5-12nm diameter), where due to their size and energy balance (gravity < particle's thermal energy) the colloidal suspension is stable in time. Those particles are usually formed by iron or cobalt oxides, covered with surfactants (oleic acid-like, the most extended) to avoid aggregation and final settling of particles. The most relevant reference is the compilation book by S. Odenbach (Odenbach, 2002), in which fluids synthesis, rheological characterization and several applications are discussed.

The MRF are similar to ferrofluids but magnetic particles are in the range of micrometres, from 1-10μm, mainly made of carbonyl iron powder, hereinafter CIP. They are strongly unstable, as a matter of fact in few minutes the particles are settled on the tank bottom. To avoid agglomeration and to have a quick restoration of homogeneous MRF, the fluid may include several additives, and in a few removing or pumping cycles the fluid can get its original behaviour.

The application of magnetic fluids in lubricated bearings was studied in some previous works with two main approaches: Hydrodynamic and hydrostatic. In the case of hydrodynamic bearings the magnetic field is applied directly into the bearing, modifying the rheology of the fluid in the pressurized thin film. The hydrostatic lubrication is based in the active restrictor that feed the bearing with controlled flowrate and pressures.

Starting with hydrodynamic lubrication, notorious changes in the Stribeck curve were observed experimentally with the use of ferrofluids (Spur and Patzwald, 1998). The use of ferrofluids in lubricated bearings design was also tackled by Osman et al., (T. A. Osman et al., 2001), focusing on the static and dynamic response (T.A. Osman et al., 2001), and the misalignment effect between shaft and bearing (Osman, 2001). A deeper approach about magnetic fluids as lubricants was developed by (Uhlmann et al., 2002) with a later application to journal bearings (Uhlmann and Bayat, 2003). More recent works in this matter (Kuzhir et al. 2011; Hsu et al. 2013), aimed at the study of the free boundary laws and the effect of surface roughness.

In the case of hydrostatic lubrication, the flowrate and pressure in a basic test bench by magnetic field under variable external loads was explored (Hesselbach and Abel-Keilhack, 2003). The same authors studied posteriorly the vibrational response of the bearings as active dampers (Díaz-Tena et al., 2013; Guldbakke and Hesselbach, 2006). Valves (or restrictors) with magnetic fluids for hydrostatic bearings determine the pressure drop in function of flowrate and applied magnetic field ((Songjing et al., 2002)). Results from different MRF and characterization of fluids in valve mode was presented in(Bin Mazlan, 2008)).

Considering that *ferrofluids* are highly stable but show very low magnetoviscous effect as bearings lubricant ((Urreta et al., 2010)); and that *MRF*, unstable but with very high magnetorheology response, the research presented in this paper was conducted exclusively with MRF. Thus,

Section 2 describes the modelling and characterization of the magnetic fluid used in the research; Section 3 deals with the mathematical modelling of the active hybrid journal bearing; Section 4 presents the prototypes for experimental validation; Section 5 summarizes the results, and finally Section 6 the main conclusions.

CHARACTERIZATION OF MAGNETORHEOLOGICAL FLUIDS

A commercial magnetorheological fluid from LORD® Corp. model MRF 122-2ED was used in this research. First at all, experimental characterization of the fluid was carried out. Data given by manufacturers are usually approximate values, both for magnetic and rheological behaviour. Therefore the fluid magnetic response was studied, along with the rheological properties under applied magnetic field and temperature.

MRFs are strongly non-Newtonian fluids, presenting a strong yield stress in function of applied magnetic field before fluid flows. The computational model to consider its behaviour was Herschel-Buckley given by Eq. (3), which is the classical Bingham model modified with thinning effect, as shown in Figure 3. Equation (4) is the apparent viscosity of the non-Newtonian fluid, the viscosity that would have a Newtonian fluid with the same shear stress (τ) at that strain rate ($\dot{\gamma}$).

[insert figure 3]

Figure 3 Models for magnetic fluids characterization.

$$\tau = \left(\tau_0(H) + K|\dot{\gamma}|^{1/m}\right)\operatorname{sgn}(\dot{\gamma}) \qquad (3)$$

$$\mu_{app} = \tau / \dot{\gamma} \qquad (4)$$

The magnetic characterization was performed with a Magnet-Physik Permagraph L magnetometer and the electromagnet EP-3, from which the magnetic field strength, flux density and magnetic fluid permeability were obtained, as shown in Figure 4. The magnetorheological characterization was carried out with a Thermo HAAKE RheoStress RS150 control stress rheometer, with a magnetic module and a thermally controlled plate.

[insert figure 4]

Figure 4 Magnetic characterization of MRF 122–2ED from LORD Corp.

Rheological analysis of the MRF was carried out, and the results are presented in Figure 5, i.e., temperature effect in viscosity and shear thinning effect in function of the magnetic field; in Figure 6, yield stress and base fluid viscosity in function of applied magnetic field at room temperature.

[insert figure 5]

Figure 5 Rheological characterization of MRF, temperature and shear thinning effect.

[insert figure 6]

Figure 6 Rheological characterization of MRF, shear stress and base viscosity.

LUBRICATION MODEL WITH MAGNETIC FLUIDS

Mathematical modelling of MRF based lubrication was carried out in this section, in order to improve the designing and optimize the behaviour of the prototypes. Modelling is focused on determining i) pressure in the fluid, ii) velocity distribution (flowrate) and iii) magnetic field in the bearing and valves. The design of the bearing and valve prototypes is discussed in Section 4, together with the test benches for experimental characterization.

Calculations and fluid simulations were carried out with two tools, in both cases considering non-Newtonian fluid: a) for two-dimensional models, modified Reynolds equation is solved into a MATLAB® based program, and b) for three-dimensional cases, computational fluid dynamics (CFD) is used with SIEMENS NX® Advanced Flow. Magnetic simulations were performed to determine the magnetic field strength and flux density with the commercial software FLUX from CEDRAT®.

Modelling was applied to two elements, described in the following two sub-sections: 1) Hybrid journal bearings and 2) magnetorheological (MR) valves.

Hybrid journal bearing lubricated with MRF

The solution of lubrication with magnetic fluids is based in a modified Reynolds equation, where the behaviour of the fluid ranges from Newtonian to non-Newtonian response. To solve the modified Reynolds equation, principles studied by (Dorier and Tichy, 1992; Tichy, 1991) were assumed, modifying the Bingham equation for the Herschel-Buckley model.

In the MRF lubrication, strong fluid yield stress requires a non-linear approach for solving the model. In this case, the shear stress in the fluid is evaluated across the gap radial section to determine the zone where the fluid is flowing and where it is plug. In Figure 7 the zones I and II are flowing; and in the zone III there is plug fluid (or pseudo-plastic MRF):

[insert figure 7]

Figure 7 Balance of forces on a fluid element in the plug region, MRF lubrication

Considering equations (1), (3), and (4), the Reynolds equation, Herschel-Buckley model and apparent viscosity respectively, the equation to solve is:

$$\frac{\partial p}{\partial \theta} = 6 \mu_{app} \rho R^2 \omega \frac{h - h^*}{h^3} \tag{5}$$

Considering the behaviour of MRF fluids, and the plug formation under magnetic field, velocity distribution of the fluid is defined with next equations, see Figure 8:

I) $$u_x(y) = \frac{1}{2}\left(-\frac{1}{K}\frac{dp}{dx}\right)\left[h_a^2 - (h_a - y)^2\right] \qquad (0 \le y \le h_a) \tag{6}$$

II) $$u_x(y) = \frac{1}{2}\left(-\frac{1}{K}\frac{dp}{dx}\right)\left[(h - h_b)^2 - (y - h_b)^2\right] \qquad (h_b \le y \le h) \tag{7}$$

III) $$u_x(y) = \frac{1}{2}\left(-\frac{1}{K}\frac{dp}{dx}\right)h_a^2 \qquad (h_a \le y \le h_b) \tag{8}$$

[insert figure 8]

Figure 8 Velocity distribution in a MRF under magnetic field with plug region (III)

Where the overall flow-rate in the bearing is:

$$Q = \left(\int_0^{h_a} u_x(0 < y < h_a)dy + \int_{h_b}^{h} u_x(h_b < y < h)dy + \int_{h_a}^{h_b} u_x(h_a < y < h_b)dy\right)L \tag{9}$$

The modified Reynolds equation is solved numerically by finite difference method, in which the bearing is discretized in "n" elements (*i x j*), and the equilibrium equation is solved (10).

$$A_0 P_{i,j} = A_1 P_{i+1,j} + A_2 P_{i-1,j} + A_3 P_{i,j+1} + A_4 P_{i,j-1} + B \tag{10}$$

Solving this equation, the pressure profile (Figure 9), the velocity distribution of the magnetic fluid in the bearing and therefore the load capacity, stiffness and flowrate were obtained.

[insert figure 9]

Figure 9 Pressure distribution (a) and gradient (b) into a journal bearing, solution in 3D graph.

Reynolds-based modelling was used for two-dimensional cases, like plain journal bearings. In the case of three dimensional models like hybrid bearings with recesses and the MR valve, the CFD tool was implemented with Herschel-Buckley model for non-Newtonian fluids, which is modified to be solved at any shear stress with a base viscosity (11). It means that below a certain shear rate value, viscosity is Newtonian and given by user (μ_0), and above that value, the viscosity is calculated for each element.

$$\mu = \mu_0 \qquad 0 \le \dot{\gamma} \le \frac{\tau_i}{\mu_0}$$
$$\mu = K + \frac{\tau_0}{\dot{\gamma}} \qquad \dot{\gamma} > \frac{\tau_i}{\mu_0} \tag{11}$$

Active magnetorheological (MR) valves

Magnetorheological (MR) valve was calculated with CFD software, where the pressure drop in the valve was determined for different flowrates and applied magnetic fields. As shown in Figure 10, the valve has a coaxial architecture with two squeeze surfaces where pressure drop and flowrate was controlled. Moreover, velocity and flowrate of the fluid were calculated as shown in Figure 10b.

Magnetic calculations were carried out to determine the magnetization of the fluid. Figure 11 shows the magnetic simulation of the MR valve, which was designed for the hybrid journal bearing, with the magnetic flux density plotted for some critical points of the valve.

[insert figure 10]

Figure 10 CFD simulations of MR valve, pressure drop (a) and flow-rate calculation (b).

[insert figure 11]

Figure 11 Magnetic simulation of MR valve (a) and magnetic field in control points (b).

DESING OF PROTOTYPE AND TEST BENCH

Being the main aim of this research the development of magnetic fluid based technology for machine-tool active spindles, two kind of devices were tested: a) magnetorheological valves for active lubrication, and b) a hybrid journal bearing with active compensation.

Magnetorheological (MR) valves

Four MR valves were dimensioned and designed to be used in the hybrid journal bearing that will be described in the next section. Each of the four valves was composed of two commercial electromagnets with coaxial architecture, in which the fluid flows through two squeeze areas where the magnetic field is concentrated. Figure 12 shows the valve and main design parameters

[insert figure 12]

Figure 12 MR valve for hybrid bearing, design sketches (a) and working principle (b).

The gap for the fluid is 0.6mm, the external diameter (D_ext) is 30mm and the internal diameter of squeeze area under magnetic field (D_int) is 24mm. Coils used in the valve had 850 turns of 0.15mm diameter wires, for a maximum 5A current, so that, as shown in Figure 11(a) the field induced in the fluid it is up to 800mT. In Figure 13 the valves and parts are shown.

[insert figure 13]

Figure 13 MR valves picture with description of parts

Hybrid journal bearing

The hybrid journal bearing demonstrator was composed by two main parts: the main structure with electric motor, main shaft and bed (the test bench), and the prototype of bearing system with monitoring and magnetic systems, see Figure 14.

[insert figure 14]

Figure 14 Sketch of hybrid journal bearing test bench and prototype

The main shaft was guided by high precision rolling bearings with runout below 2µm, and a semi-shaft was attached to be tested into the bearing, as shown in Figure 15. The shaft was driven by an electric motor, with two transmission belts. The system was clamped onto a heavy and stiff table to ensure stability. The bearing was made in bronze to ensure good tribological properties and to guide properly the magnetic field generated by two coils into the MRF. This system was mounted in the bearing house, which was guided with two perpendicular linear rolling guides to ensure two degrees of freedom between bearing and shaft, radial movement.

Load was applied radially on the bearing with a screw and a load cell (INTERFACE SM 20kN), and the displacements derived by the load were measured with two eddy current probes (Brüel&Kjaer SD-081) with a resolution below 1µm.

[insert figure 15]

Figure 15 Hybrid journal bearing test bench, overall view

[insert figure 16]

Figure 16 Hybrid journal bearing prototype, bearing house section view and dimensions

Figure 16 shows a detailed view of the bearing house and active bearing system, and the main geometrical values of the hybrid bearing and recesses.

The four magnetorheological valves shown in previous section were located close to the bearing house. Valves were working in closed-loop control with a real-time controller, INGETEAM IC3. The control diagram is shown in Figure 17. Each valve had its signal amplifiers providing up to 5A with 24V, while the fluid was pumped with a hydraulic system composed by a pump/tank module and a pressure relief valve.

[insert figure 17]

Figure 17 Active hybrid journal bearings hydraulic circuit and control

RESULTS AND DISCUSSION

The results are split into two sections: magnetorheological (MR) valves and active hybrid journal bearing.

Magnetorheological valves

Calculations were carried out with CFD due to the complexity of the flow into the channels, and they were compared with experimental results from the prototype. The first step was the calculation of magnetic field into the valve (see Figure 11), with flux density isovalues (a) and some control points in function of the current through the coils. After calculating the magnetic field values, the expected rheology of MRF was determined based on the experimental results (see Figure 5 and Figure 6). The final step was the computation in CFD of the flow rate and pressure drop in to the MR valve. To achieve right results from simulations, the viscosity for low shear rate (μ_0) was adjusted, a value selected in the computation to solve Navier-Stokes equations including Herschel-Buckley model, equation (11). A good agreement was achieved with a constant ratio in all the simulations of $\frac{\tau_0}{Q \cdot \mu_0} \approx 200$ (see Figure 18).

[insert figure 18]

Figure 18 Experimental and theoretical results in the MR valve for active bearing

Active hybrid bearing

The experimental analysis of the active hybrid journal bearing was carried out regarding three aspects: load capacity, time response and wear during operation.

Load capacity and stiffness of the active hybrid journal bearing

Load capacity and stiffness in the active hybrid bearings were experimentally studied in two ways: 1) the hydrodynamic effect improvement due to the magnetic fluid flow in the bearing, and 2) the hydrostatic response with the four MR valves feeding the recesses and working in closed loop control.

To determinate the hydrodynamic active response, the first step was to calculate the magnetic field intensity in the clearance, where the results for a half model of the system (symmetry assumption) are shown in Figure 19:

[insert figure 19]

Figure 19 Magnetic field in the hybrid bearing (a), and field strength in the gap (b) for cutting plane defined by (b), half cylinder.

With those magnetic field values and the magnetic fluid model implemented in the modified Reynolds equation (5), hydrodynamic response was evaluated for MRF, and compared with experimental results, see Figure 20 and Figure 21. The tests were carried out at two rotational speeds: 50 rpm and 200rpm.

[insert figure 20]

Figure 20 Hybrid bearing, shaft eccentricity path for 50rpm (a) and 200rpm (b).

[insert figure 21]

Figure 21 Hybrid journal bearing, load capacity for 50rpm (a) and 200rpm (b).

As shown in Figure 20 and Figure 21, magnetic fluid lubrication improves the hydrodynamic behaviour, increasing the load capacity and stiffness by at least 50% for eccentricity values around $0.4 < \varepsilon < 0.7$, and the shaft displacement was much more linear than in classical hydrodynamic bearings, with much lower cross movement.

Second experimental tests were performed to determine the system behaviour working with active hydrostatic lubrication (four MR valves), using MRF as lubricant (Figure 17). The load was applied in two directions, aligned with the recesses and at 45º, as shown in Figure 22(a), and with or without rotational speed in Figure 22 (b), hydrostatic or hydrodynamic. The lubricant pressure achieved in the hybrid bearing for the two directions is shown in Figure 23(a) and (b).

[insert figure 22]

Figure 22 Hybrid bearing, direction of the applied load (a), pressure graph with or without rotational velocity (b)

[insert figure 23]

Figure 23 Pressure distribution in the hybrid bearing for aligned (a) and 45º oriented load (b)

As presented in Figure 24, below a critical load (in function of the force direction) the stiffness of the active bearing for static loads is quasi-infinite, with typical signal noise coming from movement of the shaft (unbalance) and monitoring (signal noise), in this case <+/-5% of clearance. Once critical load is overcome, the stiffness is reduced dramatically in the case of pure hydrostatic lubrication, and in hybrid condition (200r/min in the tests) the load can be still increased due to hydrodynamic pressureFigure 24. Maximum loads were between 600N and 1200N in function of mentioned rotational velocity and applied force direction. The loads were only presented till eccentricity of 0.75, above that load/displacement the results were not reliable.

[insert figure 24]

Figure 24 Experimental results of active hybrid bearing under load, stationary values.

Time response of active hybrid journal bearing

The system time response was further tested to determine the capability of this active hybrid journal bearing for compensation of dynamic loads. The tests were carried out applying a command to the valves and measuring the movement in the shaft, obtaining the response between current in the coils and the displacement in the shaft.

[insert figure 25]

Figure 25 Experimental results of time response in active hybrid bearing.

As shown in Figure 25, the time constant of both axes was in the range of 0.06-0.07s, slight differences from hydraulic and experimental set-up. Therefore, the resulting system bandwidth (3dB point) was below 3Hz. With those values, active control by magnetic fluids cannot be considered for compensation of higher frequency perturbations. For example, in grinding or turning spindles the rotational speed is around 2000r/min, and the compensation of the shaft unbalance would require frequency around 33Hz, more than ten times higher than available in this system. But the capability to achieve quasi-infinite stiffness under static loads, and therefore maximum precision in guiding system, was demonstrated.

Bearing and shaft wear during operation

Finally, the bearing and shaft surface wear were analysed. Magnetic fluids are not optimal lubricants, since magnetic particles in suspension do not have good friction and wear properties. The effect in the surface roughness during 1000hr operation in the test bench was measured in four testing zones, as presented in Figure 26 (a) for bearing and (b) for the shaft:

[insert figure 26]

Figure 26 Wear and roughness measuring zones, a) bearing and b) shaft.

Roughness values (Ra and Rz) of the bearing and the shaft were measured in the long time test of 1000hr, with periodical measurements, leading to the values presented in Figure 27:

[insert figure 27]

Figure 27 Roughness values in the shaft, a) averaged roughness (R_a), and b) maximum roughness (R_z)

[insert figure 28]

Figure 28 Roughness values in the bearing, a) averaged roughness (R_a), and b) maximum roughness (R_z).

As shown in Figure 27 (a) and (b), the shaft roughness was not altered during the test. The bearing showed a high roughness in the zone/line labelled as 2, see **Error! Reference source not found.** (a) and (b), which was due to a scratch manipulating the bearing before the test. The roughness in the other three lines had a slight increase, which could be due to wear caused by magnetic particles in suspension.

CONCLUSIONS

The use of magnetorheological fluids as active elements in hybrid journal bearings was analysed in this research work. Some prototypes have been developed, and the validity of simulation models and the final performance of the systems were demonstrated experimentally.

- A magnetorheological fluid was experimentally analysed, obtaining deeper information about its behaviour than offered by the manufacturers; as a matter of fact, for studies in the field of magnetic fluids, such a detailed experimental characterization is highly recommended.
- Magneto-rheological valves were developed for a full prototype solution in active bearing lubrication. Good agreement between theoretical values and experimental results in terms of pressure drop and flowrate was achieved.
- An active hybrid journal bearing was developed, with active hydrodynamic effect and the use of magnetorheological valves. Hydrodynamic effect was improved around 50%, while the active hydrostatic lubrication achieved quasi-infinite static stiffness within a load range.
- Transient response of the active bearing is too slow for dynamic loads with a bandwidth lower than 5Hz. It cannot be thus used for active compensation of the unbalance in machine tool spindles shafts.

- Bearing and shaft wear rate was analysed, where a slightly roughness increment was monitored after 1000hr test in the bearing, and nothing relevant in the shaft.

REFERENCES

Aguirre, G., Al-Bender, F., Van Brussel, H., 2010. A multiphysics model for optimizing the design of active aerostatic thrust bearings. Precision Engineering 34, 507–515.

Albers, A., Nguyen, H.T., Burger, W., 2011. Energy efficient hydrodynamic journal bearing by means of closed loop controlled lubrication flow. Proceedings of ASME/STLE 2011. Presented at the IJTC2011 International Joint Tribology Conference, Los Angele, California USA.

Bassani, R., Piccigallo, B., 1992. Hydrostatic Lubrication, Tribology Series. Elsevier, Pisa University, Italy.

Bin Mazlan, S.A., 2008. The behaviour of magnetorheological fluids in squeeze mode (Thesis for PhD degree). Dublin City University. School of Mechanical and Manufacturing Engineering.

Bouzidane, A., Lakis, A.A., Thomas, M., 2008. Nonlinear Dynamic Behavior of a Rigid Rotor Supported by Hydrostatic Squeeze Film Dampers. J. Tribol. 130, 041102–041102. doi:10.1115/1.2958079

Deckler, D.C, Veillette R.J., 2004. Simulation and Control of an Active Tilting-Pad Journal Bearing. Tribology Transactions - TRIBOL TRANS 47, 440–458. doi:10.1080/05698190490463277

Díaz-Tena, E., Marcaide, L.N.L. de L., Gómez, F.J.C., Bocanegra, D.L.C., 2013. Use of Magnetorheological Fluids for Vibration Reduction on the Milling of Thin Floor Parts. Procedia Engineering, The Manufacturing Engineering Society International Conference, MESIC 2013 63, 835–842. doi:10.1016/j.proeng.2013.08.252

Dorier, C., Tichy, J., 1992. Behavior of a bingham-like viscous fluid in lubrication flows. Journal of Non-Newtonian Fluid Mechanics 45, 291–310. doi:10.1016/0377-0257(92)80065-6

Estupiñan, E.A., Santos, I.F., 2009. Linking rigid multibody systems via controllable thin fluid films. Tribology International 42, 1478–1486. doi:10.1016/j.triboint.2009.05.009

Frêne, J., Nicolas, D., Degueurce, B., Berthe, D., Godet, M., 1997. Hydrodynamic Lubrication: Bearings ans Thurst bearings, Tribology Series. Elsevier, Poitiers, France.

G. Nikolakopoulos, P., Papadopoulos, C.A., 1998. Controllable high speed journal bearings, lubricated with electro-rheological fluids. An analytical and experimental approach. Tribology International 31, 225–234. doi:10.1016/S0301-679X(98)00025-5

Guldbakke, J.M., Hesselbach, J., 2006. Development of bearings and a damper based on magnetically controllable fluids. J. Phys.: Condens. Matter 18, S2959. doi:10.1088/0953-8984/18/38/S29

Hesselbach, J., Abel-Keilhack, C., 2003. Active hydrostatic bearing with magnetorheological fluid. Journal of Applied Physics 93, 8441–8443. doi:10.1063/1.1555850

Hsu, T.-C., Chen, J.-H., Chiang, H.-L., Chou, T.-L., 2013. Lubrication performance of short journal bearings considering the effects of surface roughness and magnetic field. Tribology International 61, 169–175. doi:10.1016/j.triboint.2012.12.016

Jordan, M.A., 2000. Experimental results and implications of perturbation testing with servofluid control bearings. Orbit 2nd Quarter, 10–17.

Kuzhir, P.P., Kuzhir, P.G., Gul’kov, G.I., Rudenya, A.L., 2011. Determination of the free boundary of the lubricant layer of a ferrofluid bearing. J Eng Phys Thermophy 84, 422–429. doi:10.1007/s10891-011-0488-6

Morosi, S., Santos, I.F., 2011. Active lubrication applied to radial gas journal bearings. Part 1: Modeling. Tribology International 44, 1949–1958. doi:10.1016/j.triboint.2011.08.007

Nicoletti, R., Santos, I.F., 2008. Control System Design for Flexible Rotors Supported by Actively Lubricated Bearings. Journal of Vibration and Control 14, 347–374. doi:10.1177/1077546307080014

Nicoletti, R., Santos, I.F., 2003. Linear and non-linear control techniques applied to actively lubricated journal bearings. Journal of Sound and Vibration 260, 927–947. doi:10.1016/S0022-460X(02)00951-3

Odenbach, S., 2002. Magnetoviscous Effects in Ferrofluids, Lecture Notes in Physics. Springer.

Osman, T.A., 2001. Misalignment Effect on the Static Characteristics of Magnetized Journal Bearing Lubricated with Ferrofluid. Tribology Letters 11, 195–203. doi:10.1023/A:1012548624183

Osman, T.A., Nada, G.S., Safar, Z.S., 2001. Effect of Using Current-Carrying-Wire Models in the Design of Hydrodynamic Journal Bearings Lubricated with Ferrofluid. Tribology Letters 11, 61–70. doi:10.1023/A:1016657914947

Osman, T.A., Nada, G.S., Safar, Z.S., 2001. Static and dynamic characteristics of magnetized journal bearings lubricated with ferrofluid. Tribology International 34, 369–380. doi:10.1016/S0301-679X(01)00017-2

Peng, J., Zhu, K.-Q., 2005. Hydrodynamic Characteristics of ER Journal Bearings with External Electric Field Imposed on the Contractive Part. Journal of Intelligent Material Systems and Structures 16, 493–499. doi:10.1177/1045389X05052312

Reynolds, O., 1886. On the Theory of Lubrication and Its Application to Mr. Beauchamp Tower's Experiments, Including an Experimental Determination of the Viscosity of Olive Oil. Phil. Trans. R. Soc. Lond. 177, 157–234. doi:10.1098/rstl.1886.0005

Santos, I.F., Watanabe, F.Y., 2006. Lateral dynamics and stability analysis of a gas compressor supported by hybrid and active lubricated multirecess journal bearing. Journal of the Brazilian Society of Mechanical Sciences and Engineering 28, 485–495. doi:10.1590/S1678-58782006000400014

Shamoto, E., Suzuki, N., Hamaguchi, A., 2006. A New Fluid Bearing Utilizing Traveling Waves. CIRP Annals - Manufacturing Technology 55, 411–414. doi:10.1016/S0007-8506(07)60447-8

Songjing, L., Guanghuai, W., Dong, C., Songying, L., 2002. New type relief valve using magneto-rheological fluid.

Spur, G., Patzwald, R., 1998. Lubrication of hydrodynamic journal bearings with magnetic fluids. Production Engineering - Annals of the German Academic Society for Production Engineering (WGP) V/1, 47–51.

Sun, L., Krodkiewski, J.M., 1999. Experimental verification of modelling and analysis of the dynamic properties of an active journal bearing. 10th World congress onf the theory of machines and mechanisms, Olulu, Finland.

Tichy, J.A., 1991. Hydrodynamic lubrication theory for the Bingham plastic flow model. Journal of Rheology 35, 477–496. doi:10.1122/1.550231

Uhlmann, E., Bayat, N., 2003. Applications of ferrofluids in bearings and positioning system. Production Engineering - Annals of the German Academic Society for Production Engineering (WGP) 10, 125–128.

Uhlmann, E., Spur, G., Bayat, N., Patzwald, R., 2002. Application of magnetic fluids in tribotechnical systems. Journal of Magnetism and Magnetic Materials 252, 336–340. doi:10.1016/S0304-8853(02)00724-2

Urreta, H., Leicht, Z., Sanchez, A., Agirre, A., Kuzhir, P., Magnac, G., 2010. Hydrodynamic Bearing Lubricated with Magnetic Fluids. Journal of Intelligent Material Systems and Structures 21, 1491–1499. doi:10.1177/1045389X09356007

Weck, M., 1984. Handbook of Machine Tools. John Wiley & Sons Ltd, Chichester West Sussex ; New York.

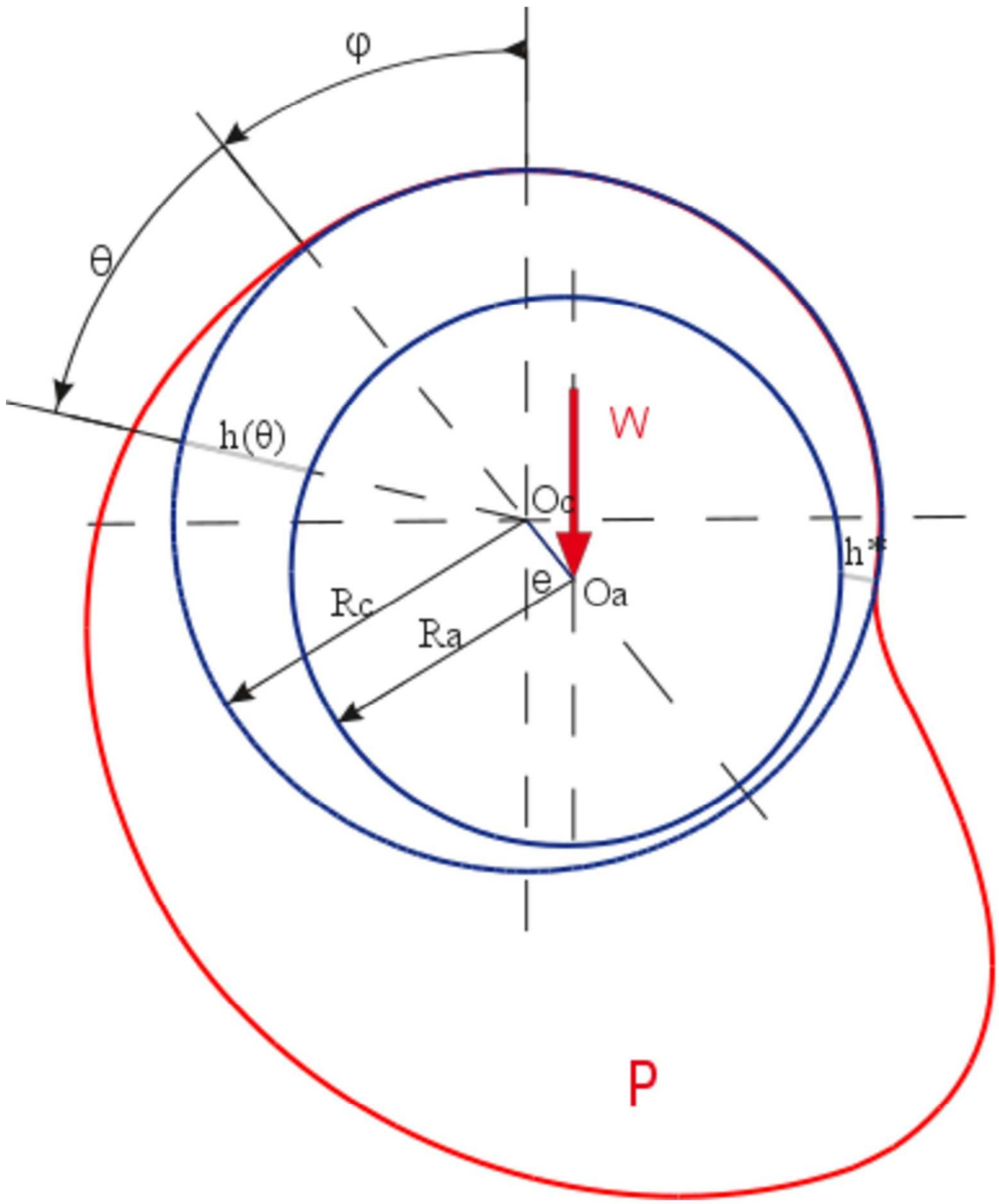

Hydrodynamic pressure in journal bearing
[insert figure 1]
130x157mm (300 x 300 DPI)

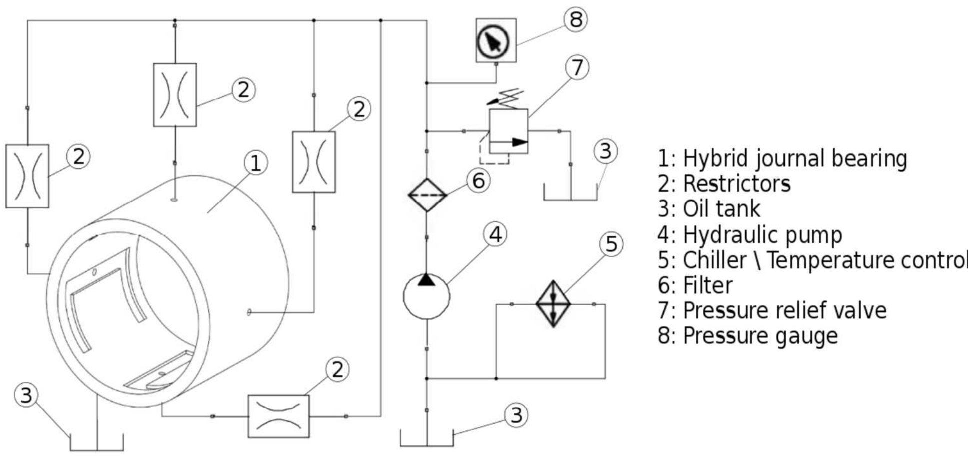

Hhybrid journal bearing and hydraulic circuit
[insert figure 2]
233x168mm (300 x 300 DPI)

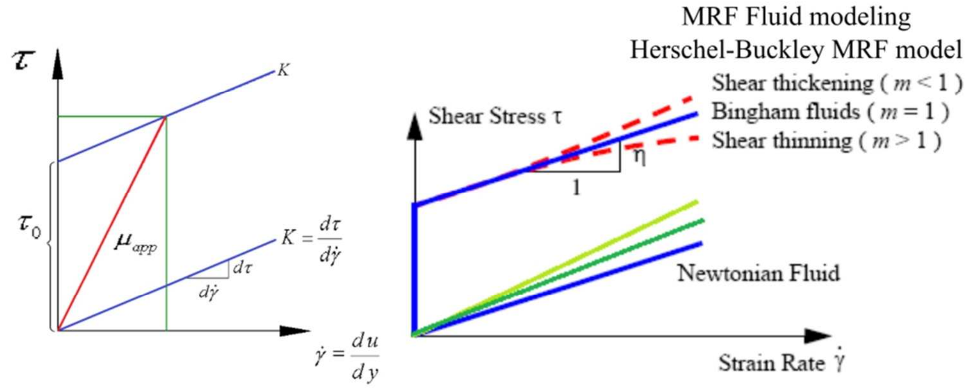

Models for magnetic fluids characterization
[insert figure 3]
111x45mm (300 x 300 DPI)

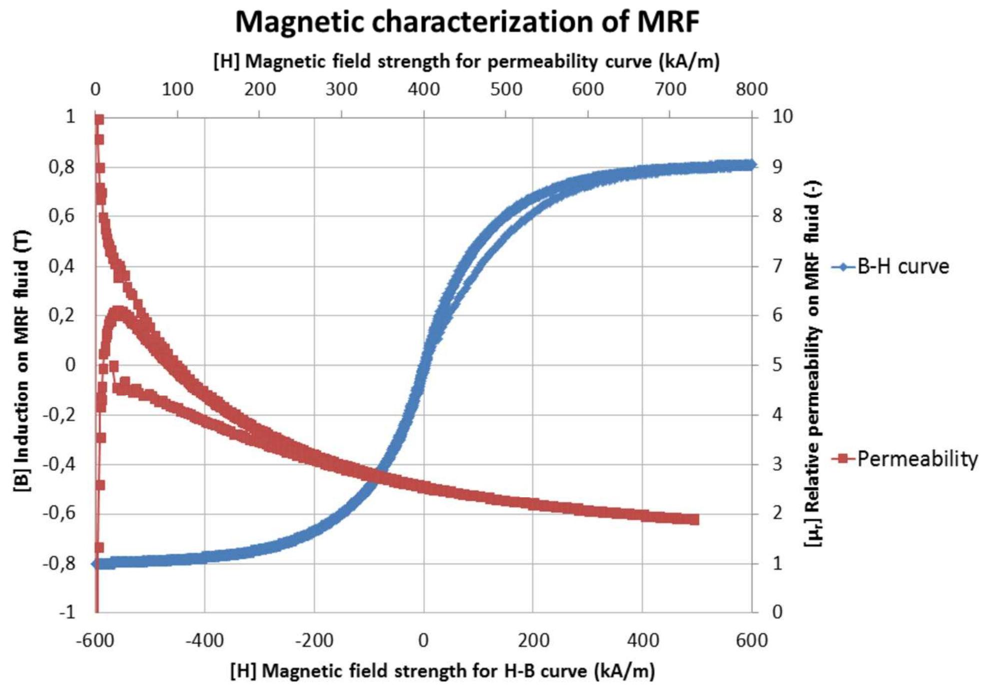

Magnetic characterization of MRF 122−2ED from LORD Corp
[insert figure 4]
192x136mm (300 x 300 DPI)

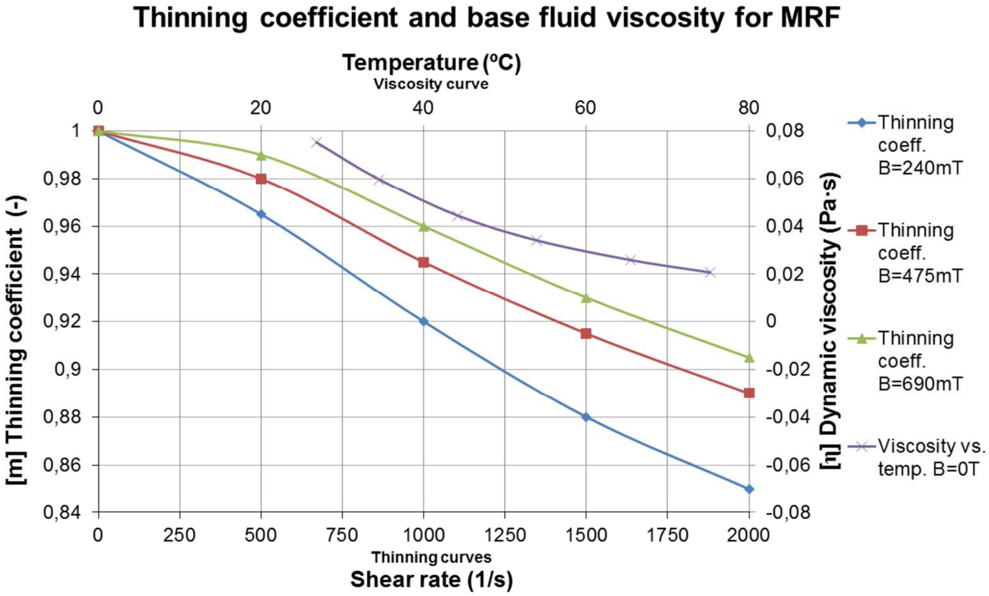

Rheological characterization of MRF, temperature and shear thinning effect
[insert figure 5]
201x124mm (300 x 300 DPI)

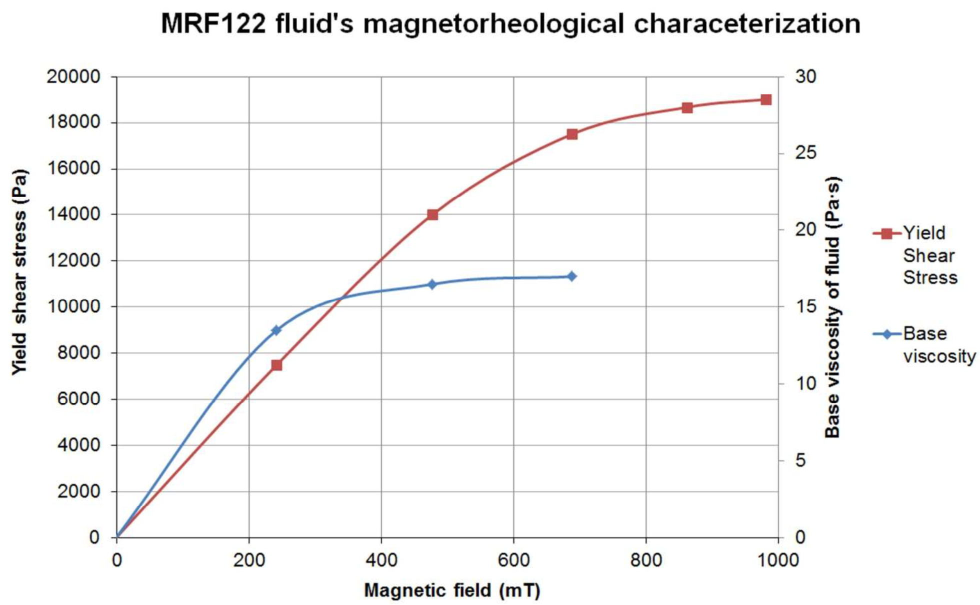

Rheological characterization of MRF, shear stress and base viscosity
[insert figure 6]
179x110mm (300 x 300 DPI)

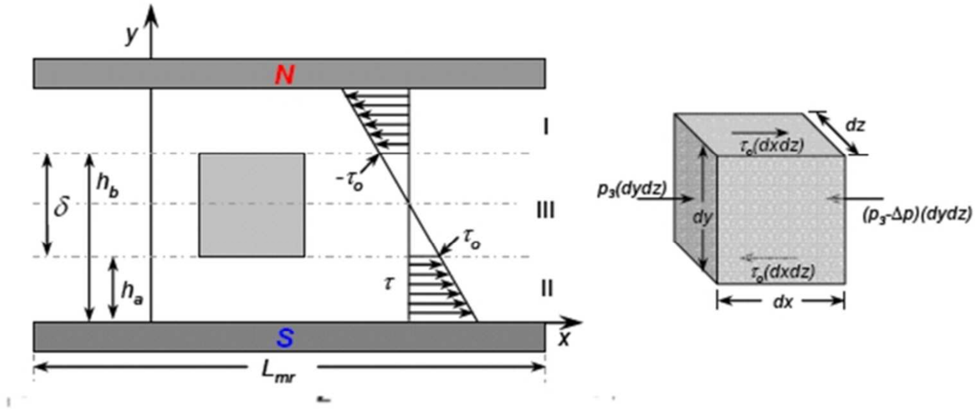

Balance of forces on a fluid element in the plug region, MRF lubrication
[insert figure 7]
63x28mm (300 x 300 DPI)

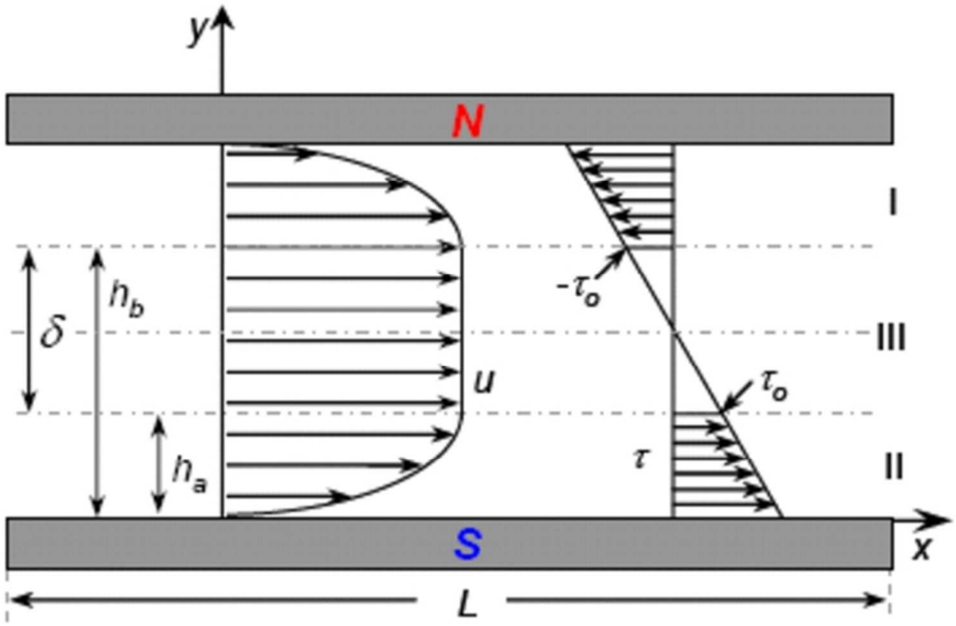

Velocity distribution in a MRF under magnetic field with plug region (III)
[insert figure 8]
57x37mm (300 x 300 DPI)

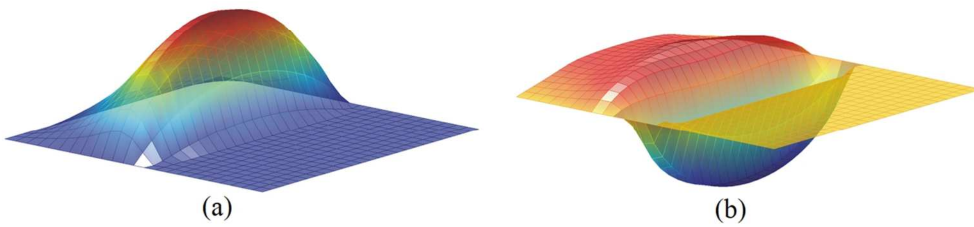

Pressure distribution (a) and gradient (b) into a journal bearing, solution in 3D graph
[insert figure 9]
131x39mm (300 x 300 DPI)

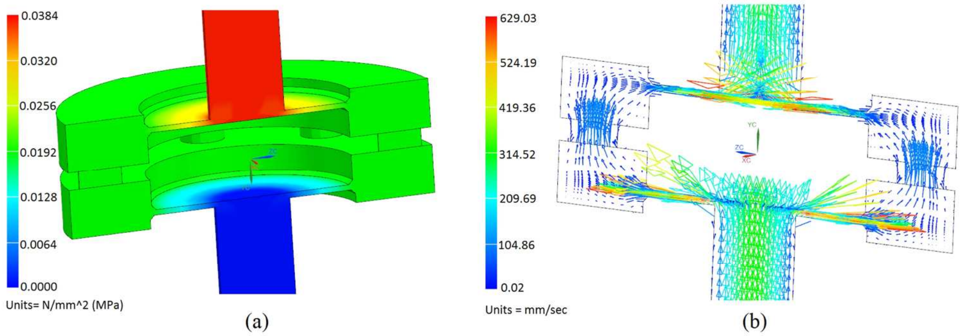

CFD simulations of MR valve, pressure drop (a) and flow-rate calculation (b
[insert figure 10]
205x76mm (300 x 300 DPI)

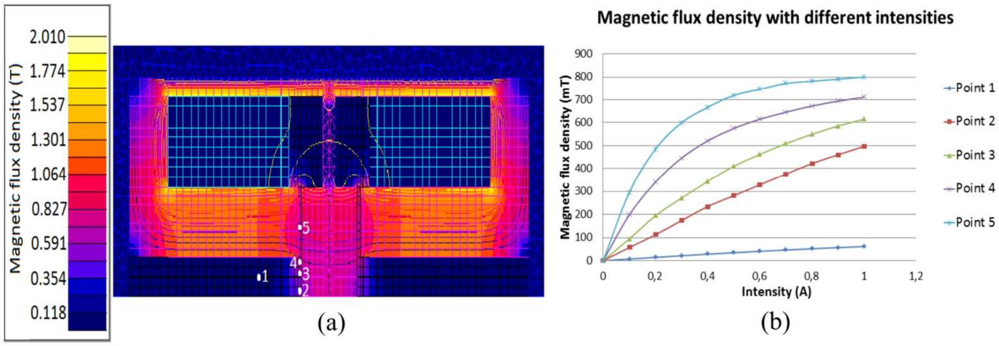

Magnetic simulation of MR valve (a) and magnetic field in control points (b)
[insert figure 11]
173x61mm (300 x 300 DPI)

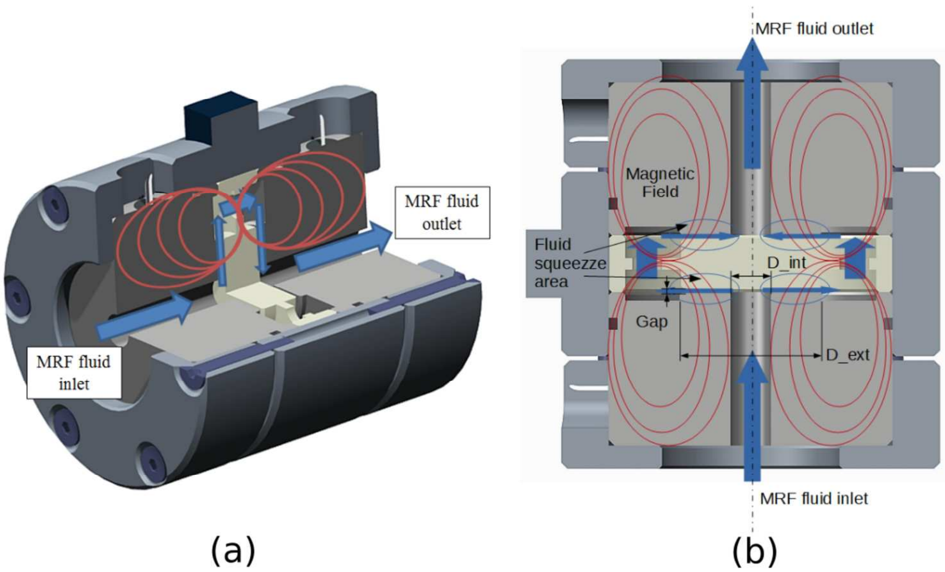

MR valve for hybrid bearing, design sketches (a) and working principle (b)
[insert figure 12]
190x107mm (300 x 300 DPI)

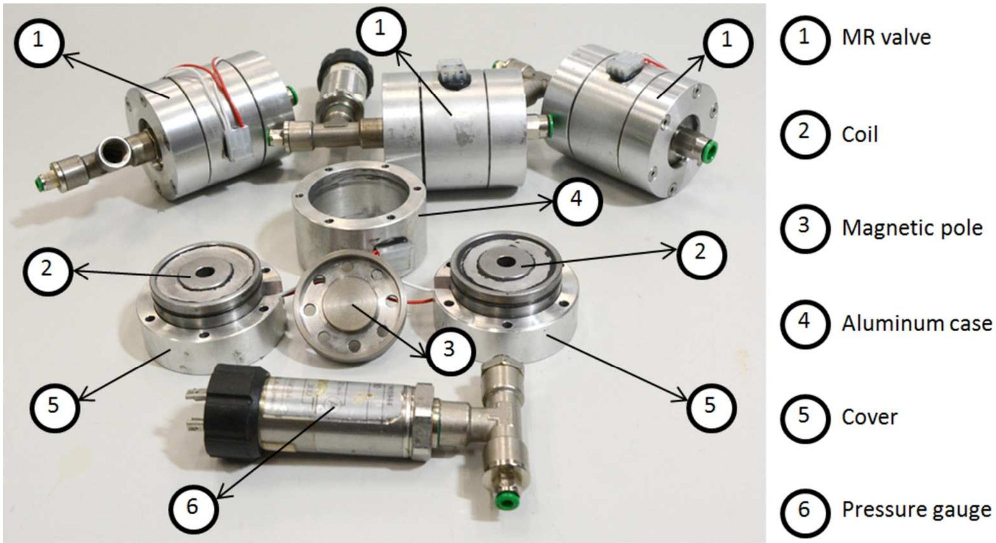

MR valves picture with description of parts
[insert figure 13]
147x80mm (300 x 300 DPI)

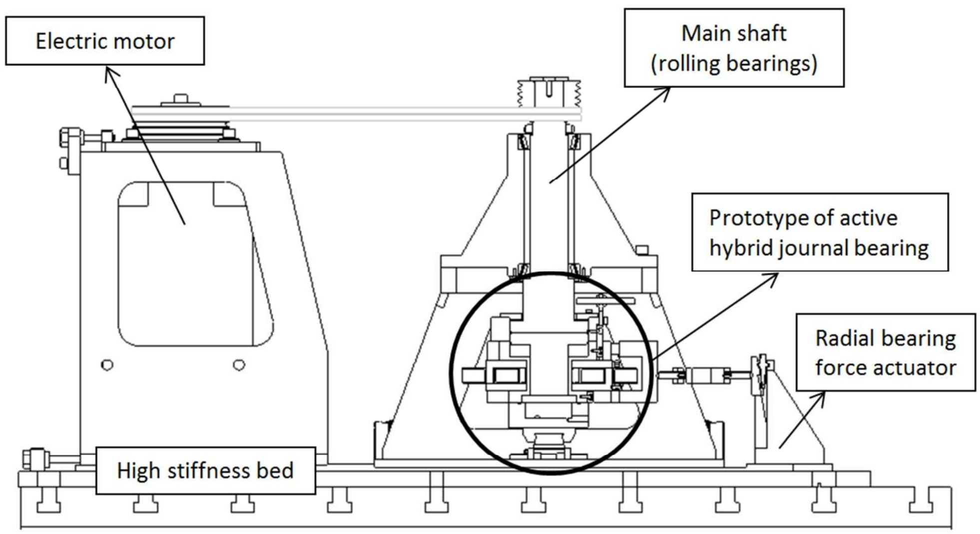

Sketch of hybrid journal bearing test bench and prototype
[insert figure 14]
166x91mm (300 x 300 DPI)

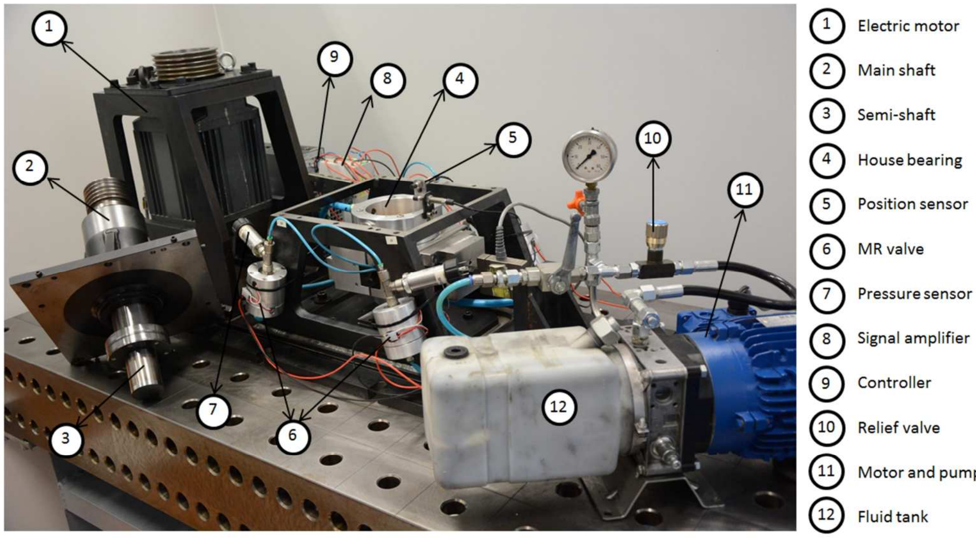

Hybrid journal bearing test bench, overall view
[insert figure 15]
180x99mm (300 x 300 DPI)

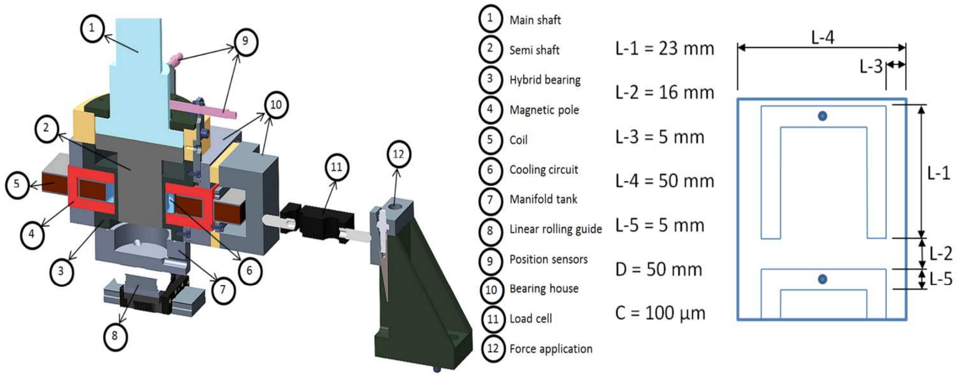

Hybrid journal bearing prototype, bearing house section view and dimensions
[insert figure 16]
221x86mm (300 x 300 DPI)

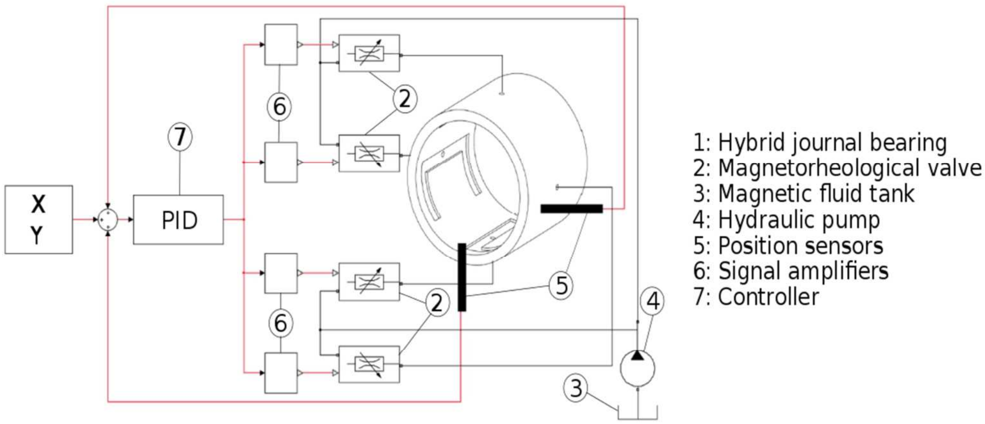

Active hybrid journal bearings hydraulic circuit and control
[insert figure 17]
138x64mm (300 x 300 DPI)

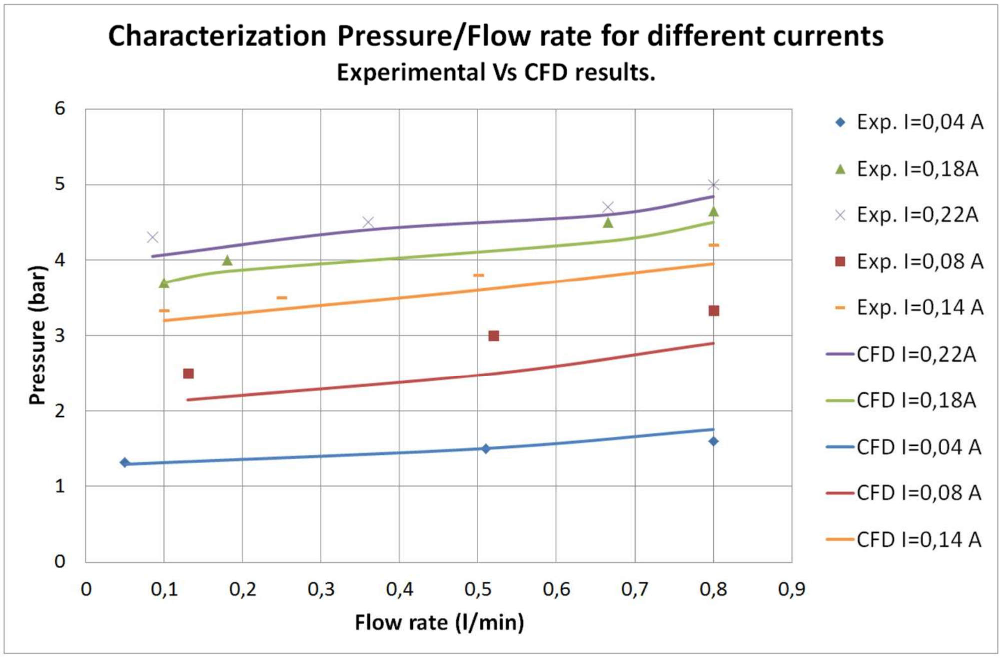

Experimental and theoretical results in the MR valve for active bearing
[insert figure 18]
231x152mm (300 x 300 DPI)

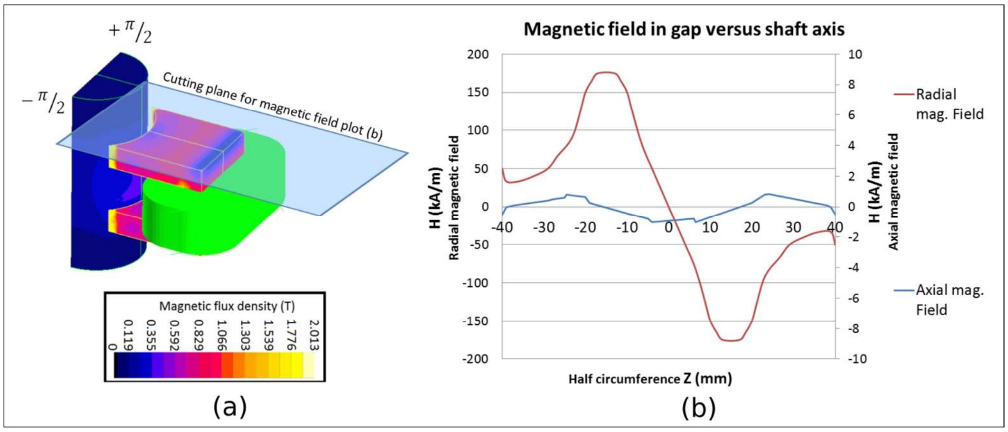

Magnetic field in the hybrid bearing (a), and field strength in the gap (b) for cutting plane defined by (b), half cylinder
[insert figure 19]
190x80mm (300 x 300 DPI)

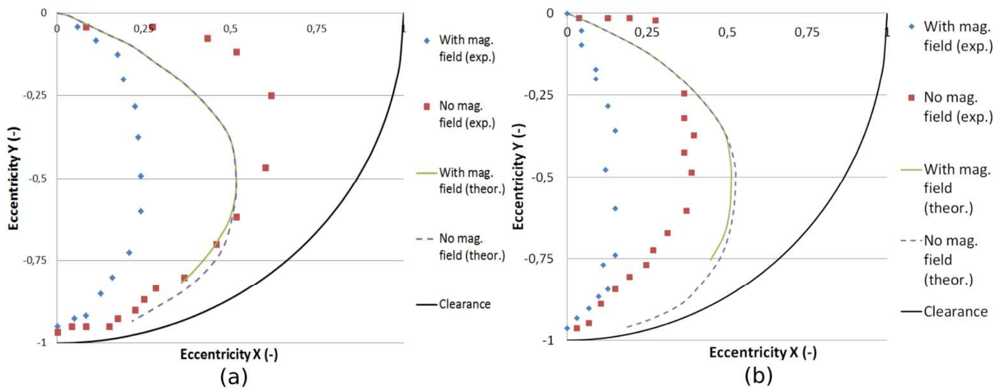

Hybrid bearing, shaft eccentricity path for 50rpm (a) and 200rpm (b)
[insert figure 20]
226x92mm (300 x 300 DPI)

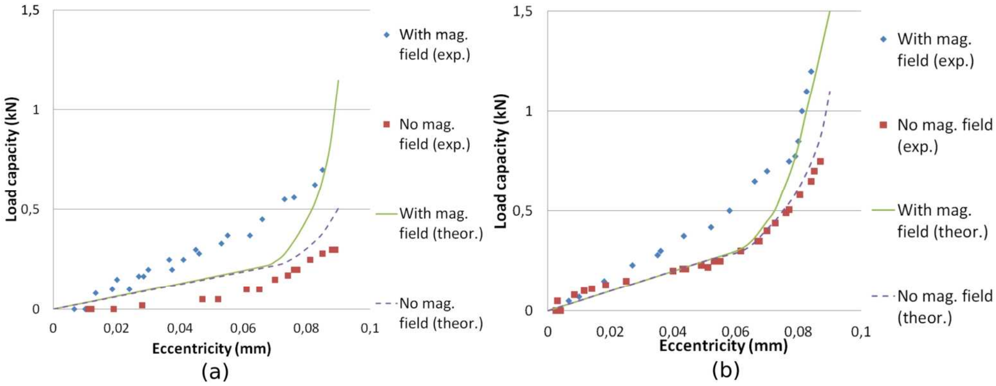

Hybrid journal bearing, load capacity for 50rpm (a) and 200rpm (b)
[insert figure 21]
214x82mm (300 x 300 DPI)

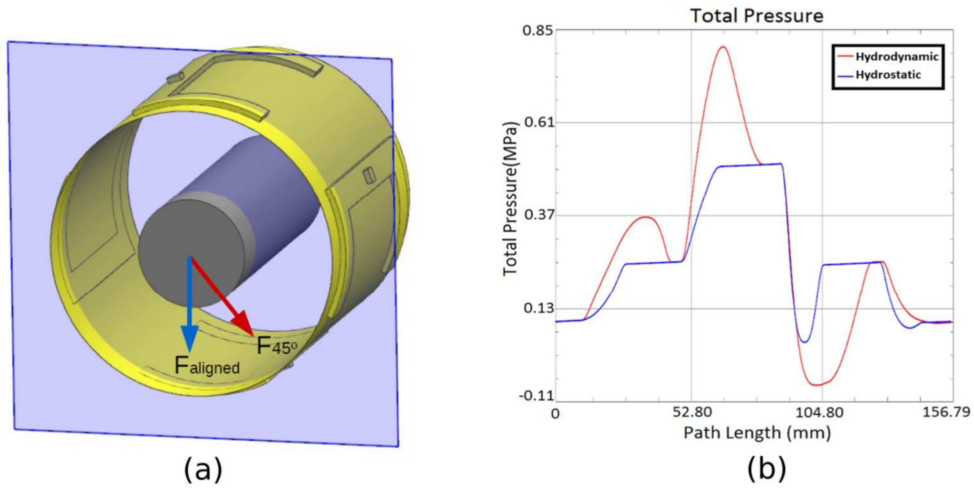

Hybrid bearing, direction of the applied load (a), pressure graph with or without rotational velocity (b)
[insert figure 22]
188x90mm (300 x 300 DPI)

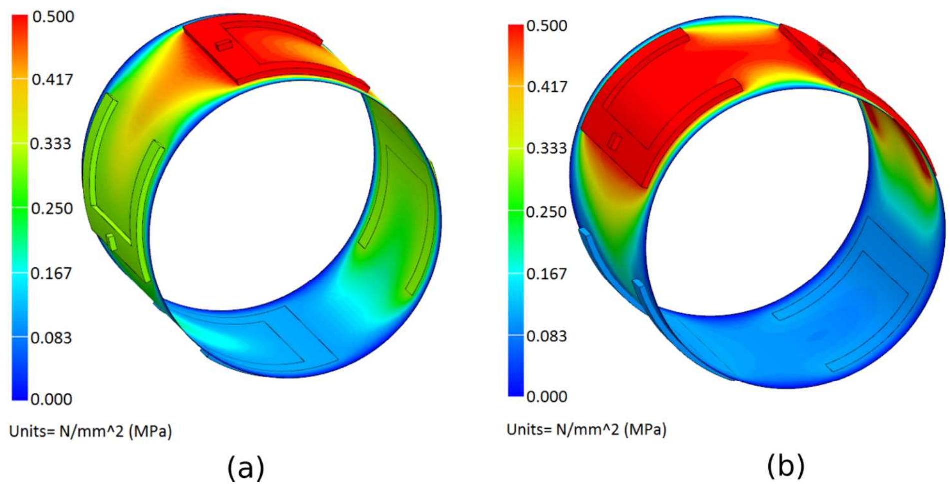

Pressure distribution in the hybrid bearing for aligned (a) and 45º oriented
[insert figure 23]
204x103mm (300 x 300 DPI)

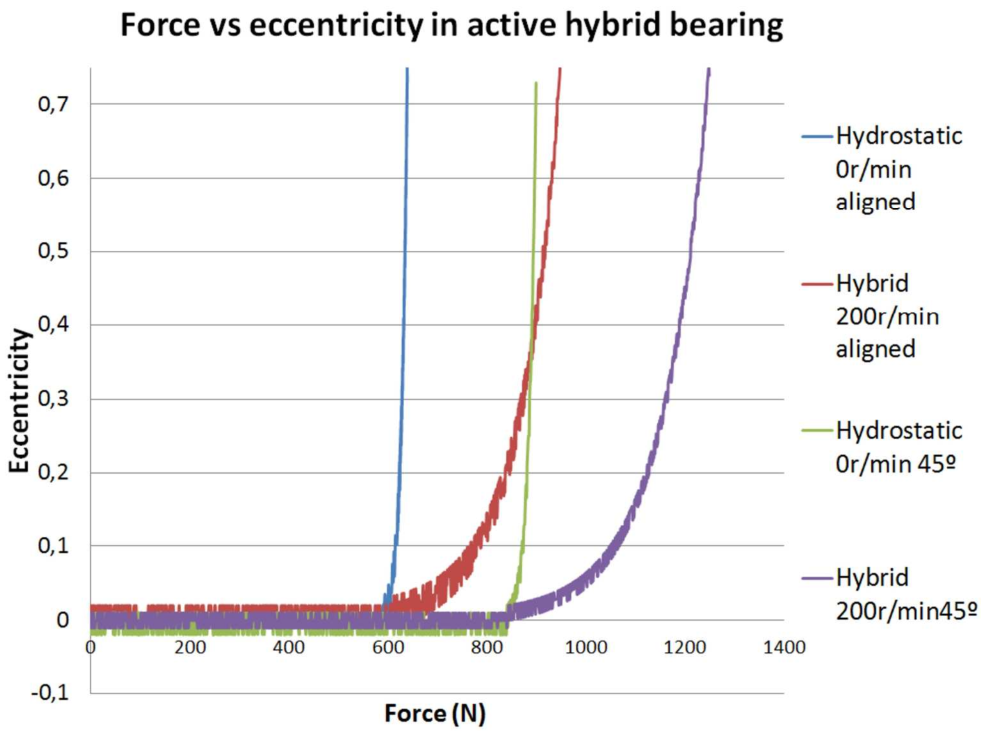

Experimental results of active hybrid bearing under load, stationary values
[insert figure 24]
198x147mm (300 x 300 DPI)

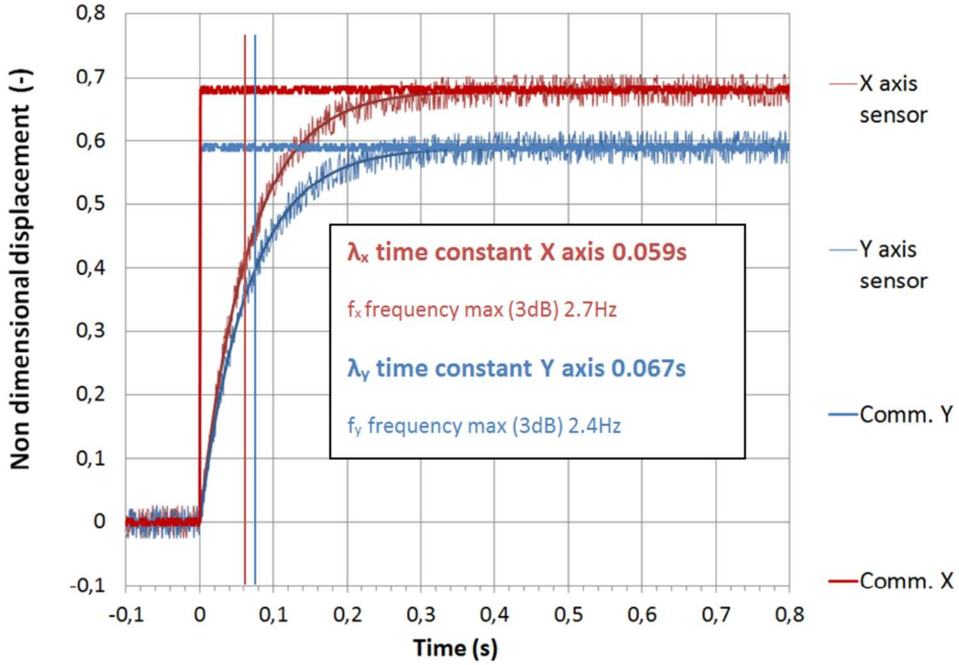

Experimental results of time response in active hybrid bearing
[insert figure 25]
184x129mm (300 x 300 DPI)

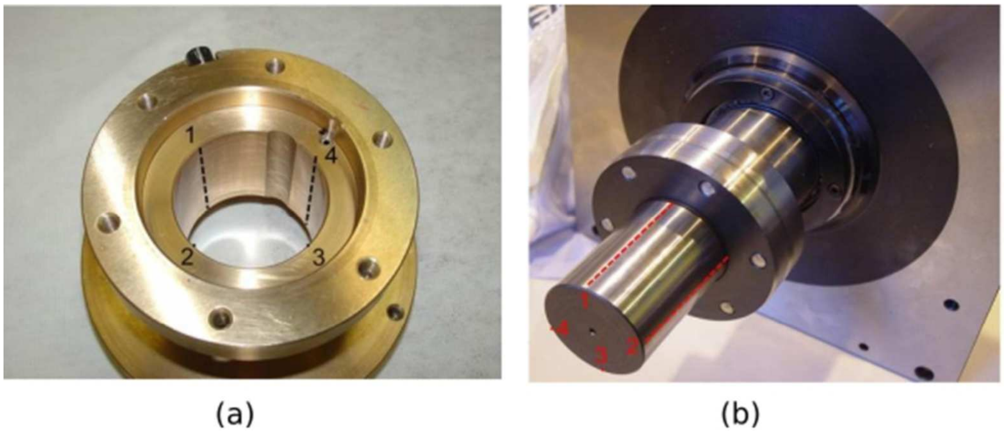

Wear and roughness measuring zones, a) bearing and b) shaft
[insert figure 26]
72x30mm (300 x 300 DPI)

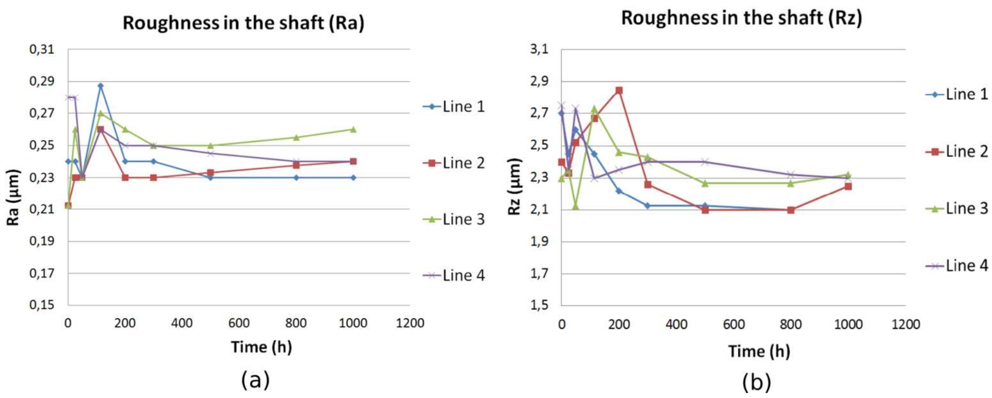

Roughness values in the shaft, a) averaged roughness (Ra), and b) maximum roughness (Rz)
[insert figure 27]
210x83mm (300 x 300 DPI)

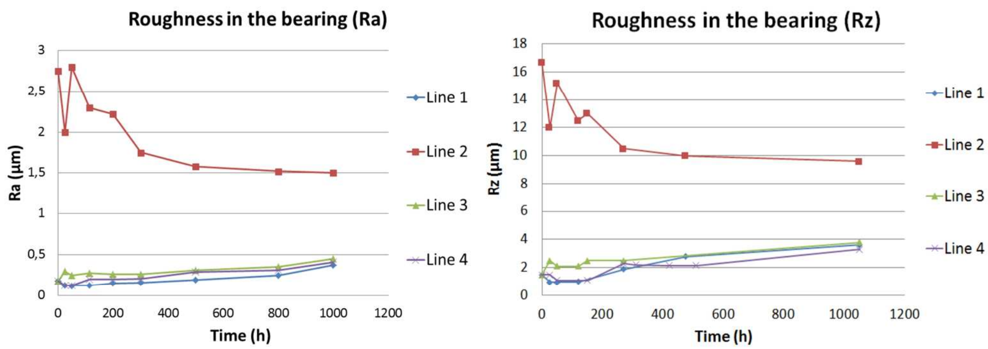

(a) (b)

Roughness values in the bearing, a) averaged roughness (Ra), and b) maximum roughness (Rz)
[insert figure 28]
178x68mm (300 x 300 DPI)